



Full Text View

[Volume 28, Issue 8 \(August 1998\)](#)

Journal of Physical Oceanography

Article: pp. 1570–1577 | [Abstract](#) | [PDF \(112K\)](#)

Observations of the Phase of Tidal Currents along a Strait

Ross Vennell

Department of Marine Science, University of Otago, Dunedin, New Zealand

(Manuscript received January 10, 1996, in final form June 22, 1997)

DOI: 10.1175/1520-0485(1998)028<1570:OOTPOT>2.0.CO;2

ABSTRACT

The phase of the M_2 surface elevation tide changes by 100° along a 40-km length of Cook Strait, New Zealand. Acoustic Doppler Current Profiler measurements are presented that show a change of only 12° in the phase of depth-averaged semidiurnal tidal currents along this same length. This phase change supports the general result developed by Vennell, which states that the phase of the cross-sectional average velocity is approximately constant along a “short” strait of variable cross-sectional area. Vennell also developed a relationship between the constant phase of tidal currents along the strait and the amplitude and phase of the surface elevation tide at the ends of a short strait. The velocity phase given by this relationship is shown to agree well with the observed tidal velocity phase in Cook Strait and one other strait.

1. Introduction

[Vennell \(1998, hereafter referred to as V98\)](#) used a scaling argument to develop a general result for oscillating barotropic flow along channels of variable cross-sectional area with linear or nonlinear dynamical balances. If a channel or strait is “short”, then the alongchannel transport is approximately nondivergent. To distinguish such channels from those that are geometrically short he used the label “nondivergently short” (ND short). He showed that in ND-short straits the alongchannel variation in the phase of the cross-sectional average velocity is small, even if the difference in elevation phase between the ends of the strait is large. V98 went on to develop a diagnostic model for tidal flow in an ND-short channel of constant width where the depth varies along the channel. From this a relationship was derived between the constant phase of the cross-sectional average alongstrait velocity and the amplitudes and phases of the surface elevation tide at the ends of the strait. This relationship is independent of the depth variation along the strait. In this paper acoustic Doppler current profiler (ADCP) measurements of the phase and amplitude of tidal currents along a 40-km section of Cook Strait are presented and the magnitude of the alongchannel variation in the phase of the velocity used to provide support for V98’s general result and ND-short strait relationship.

Table of Contents:

- [Introduction](#)
- [Measurements](#)
- [Discussion](#)
- [Conclusions](#)
- [REFERENCES](#)
- [TABLES](#)
- [FIGURES](#)

Options:

- [Create Reference](#)
- [Email this Article](#)
- [Add to MyArchive](#)
- [Search AMS Glossary](#)

Search CrossRef for:

- [Articles Citing This Article](#)

Search Google Scholar for:

- [Ross Vennell](#)

Cook Strait separates the North and South Islands of New Zealand (see [Fig. 1](#)) and is approximately 30 km wide and 200 m deep. To the north, Cook Strait is broad, flat, and approximately 100 m deep, and to the south the head of the Cook Strait Canyon falls off rapidly to 1000 m where it joins the head of the 3000-m-deep Hikurangi Trench. The 240-m-deep Terawhiti Sill joins the North and South Islands and separates the Cook Strait Canyon from the 350-m-deep Narrows Basin.

In the New Zealand region the M_2 elevation tide has an $O(1\text{ m})$ amplitude, which is five times larger than any other constituent. The M_2 tide moves as a wave in an anticlockwise direction around the continental shelf of New Zealand and results in a phase difference of 140° between the ends of the 150-km-long Greater Cook Strait ([Bye and Heath 1975](#)). Remarkably, a 100° phase difference occurs over just 40 km in the narrowest section of the strait, known as the Cook Strait Narrows ([Fig. 1](#)). This extraordinarily rapid phase variation results in strong tidal velocities of up to 300 cm s^{-1} near Cape Terawhiti ([Vennell and Collins 1991](#)). The M_2 constituent dominates tidal currents in the Strait with all other constituents having amplitudes less than 20% of the amplitude of M_2 ([Heath 1986](#); [Vennell and Collins 1991](#)).

Various techniques have been used to measure flow within Cook Strait: drift cards, electropotential ([Gilmour 1960](#)), drogues ([Sanderson 1979](#)), and even the trajectories of cross-Cook Strait swimmers ([Heath 1980](#)). Current meter measurements were made by [Heath \(1986\)](#) at three sites with meters 5 m and 50 m above the bottom ([Fig. 1](#)). After publication it was found that the data from Heath's eastern most mooring "C" had been incorrectly analyzed and consequently only his moorings "A" and "B" have been included in [Fig. 1](#). [Vennell \(1994\)](#) used a shipmounted ADCP to produce sections of the amplitude and phase of the semidiurnal tidal currents across Cook Strait at the Terawhiti Sill. [Vennell and Collins \(1991\)](#) gave tidal current observations obtained from two upward-looking ADCPs deployed for one month on the bottom of Cook Strait (see [Fig. 1](#)). Their profiles of M_2 tidal ellipse parameters exhibited a phase advance with depth and a tidal orientation that turned counterclockwise with depth in the upper water column and clockwise with depth in the lower water column. They concluded that the ellipse parameters were consistent with the superposition of the Ekman layers associated with the clockwise and counterclockwise components of the oscillating tidal current. The magnitude of the phase advance with depth (7° per 100 m) and variation in orientation (2° – 3°) were in the range expected for a model of flow driven by an oscillating pressure gradient on a rotating earth where the eddy viscosity varies linearly with depth ([Prandle 1981](#)). The moored measurements, combined in [Fig. 1](#), show that the Terawhiti Sill is approximately a line of constant phase for M_2 tidal currents.

Shipmounted ADCPs have been used to measure vertical and horizontal variation of tidal currents by several authors ([Geyer and Signell 1990](#); [Simpson et al. 1990](#); [Vennell 1994](#)). In this work, shipmounted ADCP measurements are used to examine the variation in semidiurnal tidal current ellipses along Cook Strait. These measurements complement the moored measurement in Cook Strait of [Heath \(1986\)](#), [Vennell and Collins \(1991\)](#), and the shipmounted ADCP measurements of [Vennell \(1994\)](#) made across Cook Strait.

This paper is divided into two main sections. [Section 2](#) gives ADCP measurements of semidiurnal tidal currents along Cook Strait. In the discussion in [section 3](#) the general result and ND-short strait relationship developed by V98 are applied to Cook Strait and other straits.

2. Measurements

ADCP measurements were made along a 40-km length of Cook Strait over 35 hours beginning 0002 UTC on 28 September 1991 (see [Fig. 1](#)). In order to adequately sample the semidiurnal tide, the cruise track was divided into two circuits. The northern circuit, between D1 and D3 via D2, was completed six times over 18 hours. The time taken to return to a particular part of this circuit ranged from 1.5 hours, for a point halfway between D1 and D3, and 3 hours, for points D1 and D3. After the northern circuit was completed, measurements were made on the southern circuit between D3 and D4. The southern circuit was completed six times in 17 h, giving return periods similar to those for the northern circuit.

A 150-kHz RD Instruments ADCP recorded 5-min average velocity profiles in 8-m vertical bins. The first depth bin in the velocity profile was centered 13.5 m below the surface. The rms measurement uncertainty for the ADCP was 2 cm s^{-1} . The ADCP was able to bottom track at all times. No useful measurements were returned by the ADCP in the lower 10% of the water column due to interference by the bottom. Global Positioning System satellite navigation was used to position the vessel whose speed ranged between 3 and 4 m s^{-1} .

The dataset was analyzed using a method similar to that used by [Vennell \(1994\)](#). A total of 26 points spaced 1.5 km apart were marked on the track extending north and south of the corner D2. All velocity profiles taken within 1.5 km of a particular point were considered as a time series representative of that point. The area covered by the time series at one grid point overlaps with that covered by neighboring grid points, resulting in a data smoothing along the track. Thus, the

alongtrack resolution of the time series is of order 2 km. The 26 time series were analyzed for tides using conventional methods (Godin 1972). An M_2 frequency sine wave and a mean offset were fitted to the time series, using least squares methods. The short dataset cannot resolve significant N_2 and S_2 tides within the semidiurnal band, and thus the tidal analysis for M_2 represents a composite of semidiurnal tides. These fits were made for each depth bin in the time series for which there were sufficient data (>8 points). The number of profiles in each time series was generally between 25 and 35, with up to 52 at the overlap of the two circuits. The rms value of the currents not explained by the least squares fit ranged between 10 and 27 cm s^{-1} . The standard deviations of the fitted amplitudes were typically 5 cm s^{-1} (Godin 1972), a small magnitude compared to the observed M_2 amplitudes, which were greater than 100 cm s^{-1} . Thus, the fitting process was able to clearly resolve M_2 tidal currents in the measurements. The amplitudes of the mean offsets found from the fits were only 5–10 cm s^{-1} and thus were only just resolved by the measurements.

Figure 2 shows the data and fit for a near-surface depth bin at the overlap of the two circuits, D3. The data are separated into clusters corresponding to the passage of the vessel near the overlap point. The overlap in the circuits was only 2.5 km away from one of the moored ADCPs of Vennell and Collins (1991), which was deployed on the bottom for one month at L2, 17 months prior to the ship-mounted measurements (see Fig. 1). The dashed line in Figure 2 shows the tidal predictions (based on the one-month deployment of the bottom-mounted ADCP) of near-surface currents at the moored ADCP during the time of the ship-mounted ADCP measurements. The fit to 35 hours of ship-mounted measurements agrees well with the predictions. The semidiurnal tide dominates the tidal currents, and differences between adjacent peaks in the predictions indicate that there was a small diurnal tide of amplitude 10 cm s^{-1} during the period of the ship-mounted measurements.

Figure 3 shows the results of fits to the uppermost depth bin and to the depth-averaged velocity. In calculating the depth-averaged velocity no attempt has been made to extrapolate the measurements into the bottom 10% of the water column not resolved by the ADCP. Vennell and Collins (1991) found that most of the velocity shear was confined to the lower 10% of the water column. As the velocities are weaker within the lower 10% and it constitutes only a small part of the water column, the depth average will not be significantly affected by its omission.

The near-surface semidiurnal major axis (Fig. 3a) reaches a maximum of 130 cm s^{-1} over the Terawhiti Sill, falling to approximately 100 cm s^{-1} on either side of the sill. The magnitude of the tidal ellipse minor axes were 10 cm s^{-1} north and south of the Terawhiti Sill and zero at the 23 km point just north of the sill (Fig. 3b). The sign of the minor axis indicates that the tidal velocity rotation is counterclockwise south of the sill and clockwise north of the sill. Tidal orientation (not shown) varied from 342°T in the south to 025°T in the north, paralleling the centerline of the strait.

The near-surface velocity phase lag is shown in Fig. 3c. The standard deviation of the observed phases is estimated at 3°, and thus the 90% confidence interval is estimated at $\pm 6^\circ$. The surface velocity phase lag decreases from 194° at the southern end of the line to a minimum of 184° over the Terawhiti Sill, increasing to a maximum of 204° near the northern end. The alongchannel variation in phase is approximately 20°, which occurs in about 10 km, (see Fig. 3c). Allowing for error bars of $\pm 6^\circ$ around the phase curve the measurements shows that this variation is significant.

The fit to the depth-averaged velocity is very similar to the fit to the near-surface velocity (dashed line in Fig. 3). The phase lag of the surface velocity is generally higher than that of the depth-averaged velocity (Fig. 3c). This is consistent with the phase advance with depth due to bottom friction that was observed in the moored ADCP measurements of Vennell and Collins (1991). The ship-mounted ADCP measured depth-averaged lag at D3 is 187°, compared to 210° at the ADCP moored nearby (L2 in Fig. 1). Due to the short span of the ship-mounted ADCP record it is not valid to compare the ship-mounted phase lag with the lag from the moored ADCP. However, fitting the predicted depth-averaged velocity at the moored ADCP at L2, for the 32-h shipboard measurement period, with a representative M_2 sinusoid gave an amplitude/phase lag of 120 $\text{cm s}^{-1}/180^\circ$, (cf. 132 $\text{cm s}^{-1}/187^\circ$ from shipboard measurements at D3).

The two measurement circuits were not carried out at the same time. Due to unresolved tidal constituents, in particular the diurnal tides, the semidiurnal tide measured in circuit 1 differs from the semidiurnal tide measured in circuit 2. Using tidal predictions from the moored ADCP data of 17 months earlier (L2, Fig. 1) and the same sampling and analysis procedures as for the shipboard ADCP observations demonstrated that the semidiurnal amplitudes calculated for the ship-mounted measurements in circuit 1 would be expected to be 13 cm s^{-1} greater than those in circuit 2, obtained an average of 18 h later. The ship-mounted measurements of the semidiurnal amplitudes varied by 40 cm s^{-1} , so the alongstrait variation is mainly due to spatial differences. The predictions also showed that the average phase during circuit 2 was 2° higher than the average during circuit 1. Thus, the phase lags, in Fig. 3c, north of D3 should be increased by approximately 2° to make them comparable to those south of D3. The maximum and minimum phase lags both occur in the northern circuit, so the timing of the two circuits does not affect the estimate of the alongstrait variation in phase.

3. Discussion

a. Cook Strait

The condition for a strait to be considered ND-short [V98 Eq. (8)] is well satisfied for the semidiurnal tide in Cook Strait (see [Table 1](#)). Stratification is weak in Cook Strait Narrows, with vertical variations of temperature and salinity less than 0.5°C and 0.5 psu ([Vennell 1994](#)), and consequently the flow will be nearly barotropic. Thus, the general result should be valid in Cook Strait Narrows. The ADCP measurements show that the depth-averaged velocity phase lag ranged over only 12° . The maximum and minimum lag both occur within the northern circuit, so the variation in lag is not affected by the different timing of the two circuits. The depth-averaged velocity is calculated from approximately 20 depth bins, reducing the 90% confidence interval for the phase in 1 depth bin from $\pm 6^{\circ}$ to $\pm 1.5^{\circ}$ for the depth-averaged velocity. Thus, the 90% confidence interval for the alongstrait variation in depth-averaged phase is $12^{\circ} \pm 3^{\circ}$. The measurements of [Heath \(1978\)](#) indicate that surface elevation phase varies by approximately 100° over this distance (see [Fig. 1](#) and [Table 1](#)). The smallness of the observed variation of velocity phase provides some support for the general result of V98. From [Table 1](#), the general result predicts an order 2° alongstrait variation in the phase of the cross-sectional averaged velocity in Cook Strait. Both [Vennell \(1994\)](#) and the moored results in [Fig. 1](#) demonstrate that, outside the eastern 5 km of the Terawhiti Sill, phase varies by approximately 10° with a similar variation within the eastern 5 km. Thus, the difference between the variation predicted by the general result and the observed variation may be explained by the measurements being made only along the centerline of the strait.


The general result of V98 also shows the magnitude of the transport to be approximately the same at all cross sections of a ND-short strait. Multiplying the major axes of the depth-averaged velocity for each point on the cruise track by the estimated cross-sectional area normal to the centerline of the strait showed the peak tidal transport along the strait to vary between 5 and 7 Sv ($\text{Sv} \equiv 10^6 \text{ m}^3 \text{ s}^{-1}$). The general result predicts only a 3% variation, that is, 0.2 Sv. [Vennell \(1994\)](#) showed strong flows at the eastern end of Terawhiti Sill, and thus it is not clear how well measurements made along the centerline of the strait represent the variation in transport along the strait.

The application of the ND-short strait relationship [V98, Eq. (17)] to Cook Strait Narrows is given in the lower half of [Table 1](#): $x = 0$ is at the southern end of the ADCP measurement track (D4) and $x = L$ at the northern end (D1). The elevation phase and amplitude at the ends of the track, estimated from [Heath \(1978\)](#), are also given. The difference in elevation phase along the cruise track is approximately 100° . The numerical model of Cook Strait by [Bowman et al. \(1980\)](#) uses Heath's observations to force the outer boundaries of the 150-km-long Greater Cook Strait. Their M_2 phase and amplitudes agreed well with observations given by Heath for coastal sites within Cook Strait. The cross-sectional average elevation phase and amplitude at the ends of the ADCP cruise track estimated from their model are also given in the table. The [Bowman et al. \(1980\)](#) model showed only a 60° difference in elevation phase along the cruise track. The 8-km resolution of the [Bowman et al. \(1980\)](#) model is significant compared to the 40-km-long track over which the ADCP measurements were made, and hence the phase difference estimated from [Heath \(1978\)](#) is probably more accurate. However, the estimates using the elevation phase and amplitude from both [Heath \(1978\)](#) and [Bowman et al. \(1980\)](#) yield similar values for the velocity phase lag calculated from the ND-short strait relationship given in [Table 1](#). Both of these values agree well with the observed phase lag of cross-sectional velocity estimated from the average of the phases at the moorings in [Fig. 1](#). The agreement is remarkable as the relationship is based on a very simple momentum balance. This balance neglects effects such as rotation and friction, which may be significant. [Vennell and Collins \(1991\)](#) found profiles of tidal ellipse parameters in Cook Strait Narrows consistent with the frictional effects on an oscillating current. [Table 1](#) shows frictional effects are only 10% of the acceleration, which suggests that frictional forces are observable but not important at first order. [Table 1](#) also shows that the rotational term is half the size of the acceleration term because Cook Strait Narrows is not strictly narrow. Thus differences between the phase estimated from the short strait relationship and the observed velocity phase may be due to neglecting of rotational effects.

b. Strait of Belle Isle

The Strait of Belle Isle between Labrador and Newfoundland has dimensions similar to Cook Strait Narrows and the conditions for being considered ND-short are well satisfied ([Table 1](#)). The ND-short strait model is applied between a cross section just northeast of Boat Head and a cross section at Flowers Cove. The observed elevation phase difference between the ends is 80° ([Garrett and Petrie 1981](#)), a value similar to that in Cook Strait Narrows. Estimates of cross-strait-averaged elevation phase and amplitude are given in [Table 1](#). [Garrett and Petrie \(1981\)](#) calculated the phase and amplitude of cross-sectional averaged velocity from 13 current meters deployed by [Farquharson and Bailey \(1966\)](#) on seven moorings across a section near the southwestern end of the strait. This section would correspond to $x = L$ in the ND-short strait model. After adjustment for orientation, the observed cross-sectional averaged velocity phase lag was 243° compared to 240° predicted by the ND-short strait relationship (see [Table 1](#)). [Garrett and Petrie \(1981\)](#) estimated the sizes of terms in the alongstrait momentum balance for tidal flow in the Strait of Belle Isle. They found that rotation and frictional forces were less than 20% of the acceleration and that nonlinear advection and horizontal diffusion were less than 5% of the magnitude


of the acceleration. They concluded that the dominant alongstrait momentum balance was between acceleration and pressure gradient. This is the same balance used to develop the ND-short strait relationship [V98, Eq. (17)]. Thus, the use of the ND-short strait relationship in the Strait of Belle Isle is reasonable and gives a velocity phase almost identical to the observed phase.

[Farquharson \(1962\)](#) details measurements of surface tidal streams at several sites in the strait. The measurements were made in 1906 from moored vessels at six sites covering a 45-km section of the strait. His reported M_2 current phase lags vary by only 10° along the strait, and he comments that, allowing for errors in the measurements, a constant lag of 238° would be representative throughout the strait (cf. 243° of [Garrett and Petrie 1981](#)). For the Strait of Belle Isle, the general result shows that the phase would be expected to vary of order 8° (see [Table 1](#) ) , a value comparable to Farquharson's observed variation.




Using amplitude and lags from [Farquharson \(1962\)](#) for the K_1 tide in the strait of Belle Isle, the ND-short strait relationship [V98, Eq. (17)] predicts a phase lag of 147° . The observed phase lag of the cross-sectional average K_1 velocity, after adjustment for the westward x -axis, is 137° ([Garrett and Petrie 1981](#)). The K_1 tidal stream lags within the strait reported by [Farquharson \(1962\)](#) range between 77° and 121° . The difference between these values and that of [Garrett and Petrie \(1981\)](#) may be due to difficulties in resolving a small constituent from Farquharson's short tidal records.

[Smith \(1983\)](#) deployed two current meter moorings 20 km outside the northeastern entrance to the Strait of Belle Isle. The data supplied by Smith were analyzed for tides. One current meter on one mooring and two on the other had 24-day records, that is, long enough to separate the M_2 and S_2 constituents. The eastward phase lags of the M_2 tides ranged between 228° and 260° with a mean of 248° compared to a lag of 243° at the other end of the strait. The eastward K_1 lags at Smith's moorings ranged from 190° to 209° with a mean of 200° as compared to Garrett and Petrie's 137° . Thus, the M_2 lags are comparable to, while the K_1 lags differ from, the lags at the other end of the strait. Consequently, M_2 shows a small change between the ends of the strait and may provide some support for the general result of V98. However, the K_1 lags of [Garrett and Petrie \(1981\)](#), [Farquharson \(1962\)](#), and from Smith's data are not consistent and may show a larger than expected variation along the strait.

c. Strait of Messina

The Strait of Messina between Italy and Sicily has observations dating from 800 B.C. [Bignami and Salusti \(1990\)](#) give a review of tides in the strait, which is 3 km wide and has a sill depth of only 80 m. There is a 186° change in elevation phase within only 3 km between the Ionian and Tyrrhenian Seas. At 6–13 cm, tidal amplitudes in these seas are smaller than those in either Cook Strait or the Strait of Belle Isle. However, the rapid phase change gives rise to strong tidal flow and eddies. The Strait of Messina also exhibits significant baroclinic structure. By integrating the equations of motion stepwise along the strait and allowing for changes in cross-sectional area, [Defant \(1961\)](#) calculated the velocity phase from the observed M_2 elevation phase and amplitude at the ends of the strait. He found the phase lag of the velocity to be 5.9 h. The observed velocity phase lag is 4.7 h; he attributed the difference to the effects of friction and turbulent mixing in the narrowest section of the strait. The Strait of Messina easily satisfies the conditions for a ND-short strait ([Table 1](#) ). The velocity phase calculated using the relationship [V98, Eq. (17)] is 5.8 h, almost identical to the value obtained by [Defant \(1961\)](#). The relationship is based on the same equations of motion used by [Defant \(1961\)](#), thus by exploiting the shortness of the Strait of Messina the same result can be obtained without the need to integrate the equations of motion.

d. Northumberland Strait

Northumberland Strait lies between Prince Edward Island and Nova Scotia/New Brunswick. There is an amphidromic point in the western entrance to the strait, so the general result of V98 will be applied to the eastern section of the strait between Cape Tormentine and Wood Island. Due to the 120-km length of this section and its shallow depth (20 m), \mathcal{E} for this section of the strait is 2.8 and consequently cannot be considered ND-short (see [Table 1](#) ). Therefore, the alongstrait variation in the phase of the cross-sectional average velocity should be large; the general result predicts an alongstrait variation of 140° (see [Table 1](#) ). [Farquharson \(1962\)](#) measured the phase and amplitude of the M_2 velocity in the strait. From his Fig. B2 the velocity phase lag averaged across the strait is 360° at Cape Tormentine and 230° at Wood Island. Thus, the observed variation is 130° , a value comparable to the magnitude predicted by the general result. Applying the ND-short strait relationship to this nonshort strait estimates the velocity phase lag at 279° (see [Table 1](#) ), a figure near the middle of the range of observed phases.

4. Conclusions

ADCP measurements show only a 12° variation in the phase of the depth-averaged semidiurnal tidal currents along a 40-km length of Cook Strait. The phase of the tidal elevation changes by 100° over this distance. In the Strait of Belle Isle the phase of the M_2 tidal stream varies by only 10°, while the elevation phase varies by 60°. This smallness of the variation in these two straits provides some support for the general result of V98, namely, that the phase of the cross-sectional averaged tidal velocity is approximately constant along a ND-short strait. In Northumberland Strait, which is not ND-short, the general result was able to predict the magnitude of the alongstrait variation in velocity phase.

[Vennell \(1998\)](#) developed a simple relationship between the phase of the cross-sectional average velocity, the surface elevation amplitude and phase at the ends of a ND-short and narrow strait [V98, Eq. (17)]. This relationship is independent of the strait's depth profile. The velocity phase calculated using this relationship agrees extremely well with the phase observed in the Strait of Belle Isle. There is good agreement in Cook Strait Narrows despite the significant rotational effects. In Northumberland Strait the predicted velocity phase is in the range of the observed phases. In [Fig. 4](#) contours of the relationship [V98, Eq. (17)] are plotted indicating the forcing parameters for each of the three ND-short straits considered. The ND-short strait relationship is likely to work well for tidal flows in other narrow straits where the momentum balance is between acceleration and pressure gradient.

Acknowledgments

The assistance of the officers and crew of the R/V *Rapuhia* and the staff from the New Zealand Oceanographic Institute in making the measurements is gratefully acknowledged. The New Zealand Oceanographic Institute funded the use of vessel and ADCP hire. The suggestion by an anonymous reviewer to include Northumberland Strait is greatly appreciated.

REFERENCES

- Bignami, F., and E. Salusti, 1990: Tidal currents and transient phenomena in the Strait of Messina: A review. *The Physical Oceanography of Straits*, L. J. Pratt, Ed., Kluwer Academic, 95–124..
- Bowman, M. J., A. C. Kibblewhite, and D. E. Ash, 1980: M2 Tidal effects in greater Cook Strait, New Zealand. *J. Geophys. Res.*, **85**, 2728–2742..
- Bye, J. A. T., and R. A. Heath, 1975: The New Zealand semidiurnal tide. *J. Mar. Res.*, **33**(3), 425–442..
- Defant, A., 1961: *Physical Oceanography*, Vol. 2, Pergamon Press, 598 pp..
- Farquharson, W. I., 1962: Tidal streams and currents in the Gulf of St. Lawrence. Canadian Hydrographic Service Report, Ottawa, Canada, 76 pp..
- , and W. B. Bailey, 1966: *Oceanographic study of Belle Isle Strait*. BIO Rep. 66-9, Dartmouth, Canada, 78 pp..
- Garrett, C., and B. Petrie, 1981: Dynamical aspects of the flow through the Strait of Belle Isle. *J. Phys. Oceanogr.*, **11**, 376–393..
- Geyer, W. R., and R. Signell, 1990: Measurements around a headland with a shipboard Acoustic Doppler Current Profiler. *J. Geophys. Res.*, **95**, 3189–3197..
- Gilmour, A. E., 1960: Currents in Cook Strait New Zealand. *N.Z. J. Geol. Geophys.*, **3**(3), 410–431..
- Godin, G., 1972: *The Analysis of Tides*, Liverpool University Press..
- Heath, R. A., 1978: Semidiurnal tides in Cook Strait. *N.Z. J. Mar. Freshwater Res.*, **12**, 87–97..
- , 1980: Current measurements derived from trajectories of Cook Strait swimmers. *N.Z. J. Mar. Freshwater Res.*, **14**(2), 183–188..
- , 1986: In which direction is the mean flow through Cook Strait New Zealand—Evidence for 1 to 4 week variability? *N.Z. J. Mar. Freshwater Res.*, **20**, 119–137..
- Prandle, D., 1981: On the vertical structure of tidal currents. *Geophys. Astrophys. Fluid Dyn.*, **22**, 672–677..
- Sanderson, B. G., 1979: Study of ocean circulation using radio drogues, M.Sc. thesis, Physics Dept., University of Auckland, New Zealand..
- Simpson, J. H., E. G. Mitchelson-Jacob, and A. E. Hill, 1990: Flow structure in a channel from an acoustic Doppler current profiler. *Contin. Shelf Res.*, **10**, 544–603..

Vennell, R., 1994: Acoustic Doppler current profiler measurements of tidal phase and amplitude in Cook Strait, New Zealand. *Contin. Shelf Res.*, **14**(4), 353–364..

—, 1998: Oscillating barotropic currents along short channels. *J. Phys. Oceanogr.*, **28**, 1561–1569..

—, R., and N. Collins, 1991: Acoustic Doppler current profiler measurements of tides in Cook Strait, NZ. *Proc. of 10th Australasian Conf. on Coastal and Ocean Engineering*, Hamilton, New Zealand, DSIR, 529–534..

Vercelli, F., 1925: *Crociere per lo studio dei fenomeni nello stretto di Messina*. Il regime delle correnti e delle maree nello stretto Messina. Vol. 1, Comm. Int. del Mediterraneo, Venice, Italy..

Tables

Table 1. Parameters for four sea straits and velocity phases calculated using the ND-short strait relationship [V98, Eq. (17)] and observed velocity phases. Estimates of the four terms in [V98, Eq. (8)] and ϵ are given. Sources for the observed cross-sectional average surface tidal elevation and phases and the observed current phases are ¹Heath (1978); ²Bowman et al. (1980); ³Garrett and Petrie (1981); ⁴Defant (1961) and Bignami and Salusti (1990); ⁵Heath (1986) and Vennell and Collins (1991); ⁶Vercelli (1925); and ⁷Farquharson (1962). For the Strait of Messina the phase lag in hours (as used by Defant 1961) and in degrees are given. To be consistent with the ND-short strait model geometry in Cook Strait Narrows and the strait of Messina the x -axis is northward. In the strait of Belle Isle the x axis is oriented southwest and in Northumberland Strait it is eastward. The model orientation in the strait of Belle Isle is the opposite to that used in the sources, so that the velocity phase lag was adjusted by 180° to give the bracketed observed phases.

	Cook Strait Narrows		Strait of Belle Isle		Strait of Messina		Northumberland Strait
Length, L , (m)	46	60	75	231	130	130	130
Width, W , (m)	30	20	30	3-10	25	25	25
Depth, H , (m)	150	100	100	80	50	50	50
Latitude	41°30'S		51°40'N		38°N		44°N
Continent	M_2	M_2	K_1	M_2	M_2	M_2	M_2
Elevation phase difference, ϕ_e	80°	80°	70°	168°	30°	30°	30°
Elevation amplitude ratio, α_e	0.64	0.58	0.72	0.42	0.80	0.80	0.80
Velocity ratio, α_v (m s ⁻¹)	1	0.5	0.3	2.7	0.3	0.3	0.3
$\beta \alpha_e$	0.15	0.27	0.14	0.12	1.20	1.20	1.20
Sum of terms in [V98, Eq. (8)]							
Acceleration	0.020	0.007	0.019	0.008	2.78	2.78	2.78
Advection	0.004	0.004	0.003	0.005	0.05	0.05	0.05
Rotation	0.011	0.018	0.010	0.002	0.43	0.43	0.43
Refraction ($\epsilon_e = 0.0225$)	0.002	0.006	0.002	0.004	0.04	0.04	0.04
ϵ , max of above four terms	0.020	0.007	0.019	0.008	2.78	2.78	2.78
ϵ , sum	2'	2'	2'	1'	140'	140'	140'
Elevation tide	+	+	+	+	+	+	+
Time zone relative to UTC	0	0	4	4	0	0	0
Phase lag at $x = 0$	180°	160°	220°	120°	100°/0.3	200°	200°
Amplitude lag at $x = 0$ (m)	0.35	0.40	0.21	0.065	0.66	0.47	0.47
Phase lag at $x = L$	230°	220°	207°	160°	300°/0.3	217°	217°
Amplitude lag at $x = L$ (m)	0.55	0.40	0.35	0.060	0.130	0.59	0.59
Parameters for V98, Eq. (17)							
α	0.64	1.00	0.58	0.72	0.85	0.80	0.80
β	100°	80°	75°	147°	88°/0.3	38°	38°
θ_2 from V98, Eq. (17)	60°	30°	57°	48°	88°/0.3	38°	38°
Finalized phase lag	190°	160°	240°	147°	307°/0.3	237°	237°
Observed velocity phase		204°	43°	317°	155°/0.3	230°-300°	230°-300°
Lag		204°	(347°)	(137°)			

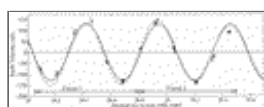
Click on thumbnail for full-sized image.

Figures



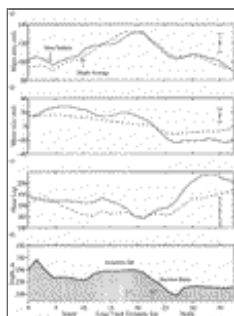
Click on thumbnail for full-sized image.

Fig. 1. Map and bathymetry of Cook Strait Narrows. Ship-mounted ADCP measurements were made along the cruise track given by the solid line joining the open circles. The cruise track consisted of two circuits, between D1 and D3 via D2 and between D3 and D4. The solid dots show the positions of moored current meters along the Terawhiti Sill. L1 and L2 are sites of the moored ADCPs of [Vennell and Collins \(1991\)](#), and L3 their current meter mooring. HA and HB are the sites of the current meter moorings of [Heath \(1986\)](#). Figures beside the solid dots give estimates of the Greenwich phase lag for depth-averaged M_2 currents. Figures inside the coastline give the Greenwich phase lag of the surface elevation M_2 tide at those sites and the dashed lines give contours of the elevation lag from [Heath \(1978\)](#).



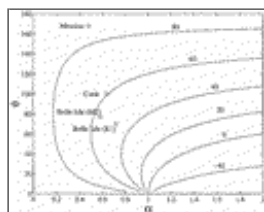
Click on thumbnail for full-sized image.

Fig. 2. Times series of northward velocity for the uppermost depth bin at the overlap of the two circuits (D3). Plus signs show the ADCP measured velocity. The solid curve gives the fit of an M_2 sinusoid to the measurements. The dashed curve gives tidal current predictions for the near-surface velocity at the nearby moored ADCP of [Vennell and Collins \(1991\)](#) at L2.



[Click on thumbnail for full-sized image.](#)

Fig. 3. Variation of tidal ellipse parameters of the semidiurnal tide along Cook Strait on 28–29 Sep 1991. (a) The amplitude of the semimajor axis (cm s^{-1}). (b) The amplitude of the semiminor axis (cm s^{-1}). Positive values indicate counterclockwise rotation and negative values clockwise rotation around the ellipse. (c) Phase lag in degrees of the major axis of the semidiurnal tide behind the equilibrium M_2 at Greenwich. (d) Water depth in meters along the measurement track. D2 gives the position of the corner in the cruise track and D3 the position of the overlap between the two circuits. In (a), (b), and (c) the solid curves give the ellipse parameters for the velocity in the uppermost ADCP bin and the dashed curve the ellipse parameters for the depth-averaged velocity. Error bars for the surface velocity are given on the right.



[Click on thumbnail for full-sized image.](#)

Fig. 4. Contours of the phase of the alongstrait cross-sectional average currents for a range of the surface elevation parameters [V98 Eq. (17)]. The x axis, α , is the ratio of the amplitudes of the elevation tide at the ends of the strait. The y axis, ϕ , is the phase difference between the elevation tide at the strait ends. The parameters for the three ND-short straits considered in this paper are indicated.

Corresponding author address: Dr. Ross Vennell, Department of Marine Science, University of Otago, Box 56, Dunedin, New Zealand.

E-mail: vennell@otago.ac.nz

[top ▲](#)



© 2008 American Meteorological Society [Privacy Policy and Disclaimer](#)
 Headquarters: 45 Beacon Street Boston, MA 02108-3693
 DC Office: 1120 G Street, NW, Suite 800 Washington DC, 20005-3826
amsinfo@ametsoc.org Phone: 617-227-2425 Fax: 617-742-8718
[Allen Press, Inc.](#) assists in the online publication of AMS journals.